C. R. Mecanique 346 (2018) 89–97

Contents lists available at ScienceDirect

Comptes Rendus Mecanique

www.sciencedirect.com

Impact of local diffusion on macroscopic dispersion in three-dimensional porous media

Arthur Dartois, Anthony Beaudoin *, Serge Huberson

Institut Pprime, SP2MI – Téléport 2, boulevard Marie-et-Pierre-Curie, BP 30179, 86962 Futuroscope Chasseneuil cedex, France

ARTICLE INFO

Article history:
Received 20 March 2017
Accepted 1 December 2017
Available online 17 January 2018

Keywords:
Dispersion
Diffusion
Covariance function
Lagrangian velocity
Tracker method
Monte Carlo approach

ABSTRACT

While macroscopic longitudinal and transverse dispersion in three-dimensional porous media has been simulated previously mostly under purely advective conditions, the impact of diffusion on macroscopic dispersion in 3D remains an open question. Furthermore, both in 2D and 3D, recurring difficulties have been encountered due to computer limitation or analytical approximation. In this work, we use the Lagrangian velocity covariance function and the temporal derivative of second-order moments to study the influence of diffusion on dispersion in highly heterogeneous 2D and 3D porous media. The first approach characterizes the correlation between the values of Eulerian velocity components sampled by particles undergoing diffusion at two times. The second approach allows the estimation of dispersion coefficients and the analysis of their behaviours as functions of diffusion. These two approaches allowed us to reach new results. The influence of diffusion on dispersion seems to be globally similar between highly heterogeneous 2D and 3D porous media. Diffusion induces a decrease in the dispersion in the direction parallel to the flow direction and an increase in the dispersion in the direction perpendicular to the flow direction. However, the amplification of these two effects with the permeability variance is clearly different between 2D and 3D. For the direction parallel to the flow direction, the amplification is more important in 3D than in 2D. It is reversed in the direction perpendicular to the flow direction.

1. Introduction

Macroscopic dispersion is a key component of solute transport in geological media and is highly influenced by the heterogeneity of geological media ([1], [2]). It is essentially due to its relation to the statistics of flow velocity fields, which has been demonstrated with the first analytical expressions linking velocity and dispersion, given in stratified formations by Matheron et al. [3] and in porous formations by Dagan [4,5], Gelhar et al. [6] and Winter et al. [7].

In his work [8–10], Dagan showed by using the Taylor's work [11] and a Lagrangian framework that the dispersion tensor $D_{t,ij}$ at time t is linked to the auto-covariance tensor C_{ij} of the total displacement $\mathbf{X}_t$:

$$D_{t,ij} = \frac{1}{2}\frac{\mathrm{d}C_{ij}(\mathbf{X}_t)}{\mathrm{d}t} \quad \text{with} \quad C_{ij}(\mathbf{X}_t) = E[\mathbf{X}'_{t,i}\mathbf{X}'_{t,j}] \tag{1}$$

* Corresponding author.
E-mail address: anthony.beaudoin@univ-poitiers.fr (A. Beaudoin).

https://doi.org/10.1016/j.crme.2017.12.012

where $\mathbf{X}'_t = \mathbf{X}_t - E[\mathbf{X}_t]$ is the total displacement fluctuation. Starting its motion at the position $\mathbf{X}_0$ and time t_0, the total displacement of a particle is given by:

$$\mathbf{X}_t(t;\mathbf{X}_0,t_0) = \mathbf{X}(t;\mathbf{X}_0,t_0) + \mathbf{X}_d(t;t_0) \tag{2}$$

The advection displacement $\mathbf{X}$ is related to the flow velocity $\mathbf{u}$:

$$\mathbf{X}(t;\mathbf{X}_0,t_0) = \mathbf{X}_0 + (t-t_0)\mathbf{i} + \int_{t_0}^{t} \mathbf{u}(\mathbf{X}_t)\,\mathrm{d}t' \tag{3}$$

where $\mathbf{i}$ is an unit vector in the x direction. Being a Brownian motion defined by a zero mean and a normal pdf, the local dispersion displacement $\mathbf{X}_\mathrm{d}$ is uncorrelated with $\mathbf{u}$. Then, $C_{ij}(\mathbf{X}_t)$ can be given by:

$$C_{ij}(\mathbf{X}_t) = C_{ij}(\mathbf{X}) + 2(t-t_0)D_{\mathrm{d},ij} \tag{4}$$

where $D_{\mathrm{d},ij}$ is the local dispersion tensor. If diffusion is only considered, $D_{t,ij}$ can be written as:

$$D_{t,ij} = \frac{1}{2}\frac{\mathrm{d}C_{ij}(\mathbf{X})}{\mathrm{d}t} + D_\mathrm{m}\delta_{ij} \quad \text{with} \quad C_{ij}(\mathbf{X}) = \int_{t_0}^{t}\int_{t_0}^{t} C_{ij}(\mathbf{V})\,\mathrm{d}t'\,\mathrm{d}t'' \tag{5}$$

with D_m the diffusion coefficient, δ_{ij} the Kronecker symbol and $C_{ij}(\mathbf{V})$ the Lagrangian auto-covariance tensor computed from the velocity sampled by the particles undergoing diffusion. The previous equation can be re-written as:

$$D_{t,ij} = \frac{1}{2}\int_{t_0}^{t} C_{ij}(\mathbf{V})\,\mathrm{d}t' + D_\mathrm{m}\delta_{ij} \tag{6}$$

This equation clearly shows the role played by diffusion. In addition to participating in the spreading of particles, diffusion modifies the sampling of the Eulerian velocity by the particles. Then, the analysis of the influence of diffusion on dispersion depends on the estimation of the Lagrangian auto-covariance tensor. Following the analytical approach and under simplification assumptions, this auto-covariance tensor can be expressed with different methods such as the Corsin's conjecture ([9], [12], [13]) and the perturbation theory ([10], [14], [15]). However, the analytical solution only gives valid results for weakly heterogeneous permeability fields ([16]). While the numerical approach does not require an approximation of the velocity auto-covariance tensor except in some cases ([17]), it is still confronted with convergence issue at higher values of heterogeneity, especially in 3D, and the macroscopic dispersion coefficients do not always reach an asymptotic value as described in a Fickian regime ([18], [19], [20]). While in these works, the macroscopic dispersion coefficients are computed through the particle positions and the second-order moments, equation (6) enables the macroscopic dispersion coefficients to be calculated from the Lagrangian velocity covariance. This method has been used in Salandin et al. [21] and later Gotovac et al. [22] with Monte Carlo simulations where particles are tracked but are limited to pure advection cases in isotropic 2D heterogeneous porous media.

In this work, we compute the Lagrangian velocity covariance functions for pure advection and diffusion cases in isotropic highly heterogeneous 2D and 3D porous media. To obtain a well-defined covariance function, we use high performance computing with the numerical model PARADIS, PARAllel DISpersion, available in the software platform H2OLAB (http://h2olab.inria.fr/) to compute the particles trajectories. PARADIS performs large-scale and finely resolved Monte Carlo simulations for estimating the trajectory of inert particles in heterogeneous porous media characterized by an exponentially correlated log-normal isotropic permeability fields ([23,24], [25,20]). These previous works focus on advective and diffusive conditions in 2D and purely advective in 3D. Furthermore, the macroscopic coefficients are computed through the temporal derivation of particle cloud second-order moments. This work introduces the effect of diffusive condition and a numerical analysis of Lagrangian velocity covariance functions, which allows the identification of the impact of local diffusion on dispersion in 2D and 3D.

2. Covariance function computing

The covariance function C_{ii} of the component V_i of the Lagrangian velocity $\mathbf{V}$ can be estimated as follows:

$$C_{ii}(\mathbf{V}) = \sigma^2_{V_i} - \gamma_{V_i}(h) \tag{7}$$

where $\sigma^2_{V_i}$ and γ_{V_i} are the variance and variogram of V_i respectively; h represents the time step between two times. To compute γ_{V_i}, the stochastic variable V_i has to respect two properties:

Table 1
Characteristics of the numerical simulations performed for estimating the Lagrangian velocity covariance functions in 2D and 3D heterogeneous porous media.

Source	N_P	N_S	$L_X \times L_Y \times L_Z$
Salandin et al. [21]	40	500	$64\lambda \times 64\lambda \times 0\lambda$
Gotovac et al. [22]	4,000	500	$64\lambda \times 128\lambda \times 0\lambda$
Present work in 2D	10,000	100	$204.8\lambda \times 102.4\lambda \times 0\lambda$
Present work in 3D	10,000	100	$51.2\lambda \times 25.6\lambda \times 25.6\lambda$

- the expected value of the component V_i is not time dependent,

$$\forall t \in \mathbb{R},\ E[V_i(t)] = M \quad \text{with } M \text{ a constant} \tag{8}$$

- the covariance function $C_{ii}(\mathbf{V})$ is stationary up to the second order,

$$\forall (t,h) \in \mathbb{R}^2,\ C_{ii}(\mathbf{V}) = C(V_i(t), V_i(t+h)) = C_{ii}(h) \tag{9}$$

From a practical point of view, the variogram γ_{V_i} represents the half-variance Var between two values of the component V_i of the Lagrangian velocity $\mathbf{V}$, taken at two times t and $t+h$:

$$\gamma_{V_i}(h) = \frac{1}{2}\mathrm{Var}[V_i(t) - V_i(t+h)] = \frac{1}{2}E[(V_i(t) - V_i(t+h))^2] \tag{10}$$

The discrete form of the previous equation reads:

$$\gamma_{V_i}(h) = \frac{1}{2N(h)} \sum_{j=1}^{N(h)} (V_i(t) - V_i(t+h))^2 \tag{11}$$

with $N(h)$ the number of pairs V_i whose time is separated by h. Considering the number of particles N_P and the number of Monte Carlo simulations N_S, the discrete form of $C_{ii}(\mathbf{V})$ is given by:

$$C_{ii}(\mathbf{V}) = \sum_{q=1}^{N_S} \left[\sum_{k=1}^{N_P} \left(\sigma_{V_i}^2 - \frac{1}{2N(h)} \sum_{j=1}^{N(h)} [V_i(t) - V_i(t+h)]^2 \right) \right] \tag{12}$$

This equation is composed of two means that have to be calculated for the estimation of the covariance function $C_{ii}(\mathbf{V})$. The first mean is performed on a number of particles $N_P = 10{,}000$, and the second mean on a number of Monte Carlo simulations $N_S = 100$. Thus, the resulting covariance function $C_{ii}(\mathbf{V})$ is estimated by means of 10^6 particle variograms. The particles were tracked in computational domains of dimensions $204.8\lambda \times 102.4\lambda$ in 2D and $51.2\lambda \times 25.6\lambda \times 25.6\lambda$ in 3D with a correlation length of heterogeneous permeability fields, $\lambda = 10$ m. For the sake of comparison, Table 1 gives the numerical parameters used by Salandin et al. [21] and Gotovac et al. [22] in their 2D works. It should also be noted that the Lagrangian velocity covariance functions are equal in the directions perpendicular to the flow direction because the heterogeneous permeability fields are assumed to be isotropic. In the following sections, the Lagrangian velocity covariance functions will be noted $C_{11}(\mathbf{V}) = C_L(h)$ (L, longitudinal for the direction parallel to the flow direction) and $C_{22}(\mathbf{V}) = C_{33}(\mathbf{V}) = C_T(h)$ (T, transverse for the directions perpendicular to the flow direction).

3. Covariance function validation

Englert et al. [26] gave a synthesis of previous works using a Monte Carlo analysis and covariance computation for studying flow velocity fields in 3D porous media characterized by isotropic and anisotropic heterogeneous permeability fields. These previous works have shown that the analytical approximations of Eulerian velocity covariance functions under pure advection conditions are validated until the permeability variance σ^2 exceeds 1 for the first order and 2 for the second order, with 3D isotropic heterogeneous permeability fields ([27], [28], [29], [30], [31]) and 3D anisotropic fields ([32], [33]). Englert et al. [26] indicated that the validity of second-order approximations estimating the Eulerian velocity covariance functions is still an unresolved issue.

Fig. 1 shows the longitudinal (C_L, top) and transverse (C_T, bottom) covariance functions obtained with the first-order approximation given by Russo [34], the Monte Carlo analysis used by Englert et al. [26] and the present method for a permeability variance $\sigma^2 = 1$ with a purely advection condition in 3D. The covariance functions are adimensionalized with the variances of flow velocity components, σ_L^2 and σ_T^2, respectively in the longitudinal and transverse directions. For an isotropic heterogeneous permeability field, the equations of Eulerian velocity covariance functions obtained with the first-order approximation ([35]) are:

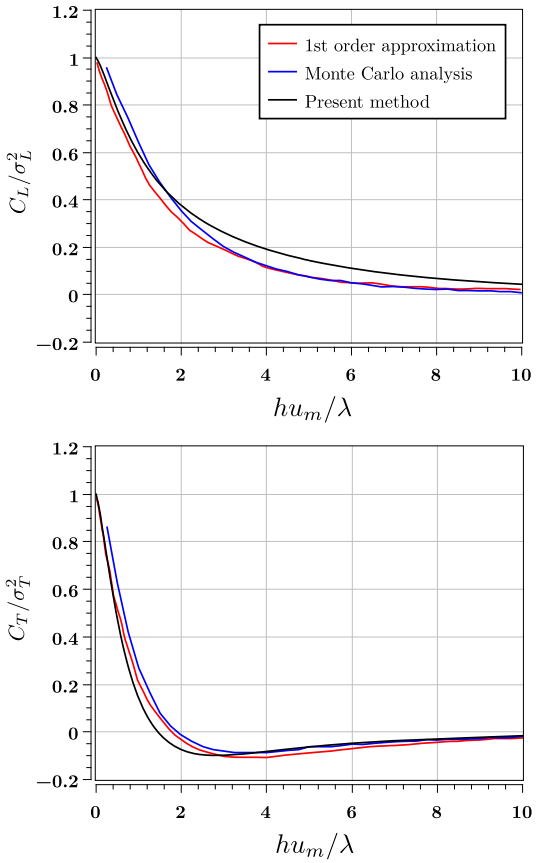

Fig. 1. Longitudinal (C_{L}, top) and transverse (C_{T}, bottom) covariance functions obtained with the first order approximation given by Russo [34] (red line), the Monte Carlo analysis used by Englert et al. [26] (blue line) and the present method (black line) for a permeability variance $\sigma^2 = 1$ with a purely advection condition in 3D.

- in the longitudinal direction,

$$\frac{C_{\mathrm{L,1st}}(h)}{\sigma^2_{\mathrm{L,1st}}} = \sigma^2 u_{\mathrm{m}}^2 \exp(-\sigma_{\mathrm{L}}^2 h u_{\mathrm{m}}/\lambda) \tag{13}$$

- in the transverse direction,

$$\frac{C_{\mathrm{T,1st}}(h)}{\sigma^2_{\mathrm{T,1st}}} = \sigma^2 u_{\mathrm{m}}^2 (1 - h u_{\mathrm{m}}/(2\lambda)) \exp(-h u_{\mathrm{m}}/(2\lambda)) \tag{14}$$

u_{m} denotes the mean flow velocity.

Both numerical approaches give results similar to the first-order approximation in the two directions. The global behaviour of two covariance functions, C_{L} and C_{T}, is correctly simulated with the Monte Carlo analysis used by Englert et al. [26] and the present method. As it was noted in the work by Salandin et al. [21], the Lagrangian and Eulerian velocity covariance functions are very close.

The influence of the particle number N_{P} on the accuracy of the present method has been investigated. In Fig. 2, the covariance functions obtained with the present method have been plotted for a particle number N_{P} ranging from 2,500 to 15,000 in 3D with a permeability variance $\sigma^2 = 2.25$ and a purely advection condition. The convergence is quickly established in both transverse and longitudinal directions, and is reached for $N_{\mathrm{P}} > 5{,}000$.

Fig. 3 shows the longitudinal (σ^2_{L}, top) and transverse (σ^2_{T}, bottom) variances of flow velocity fields as functions of the permeability variance σ^2 in 3D with a purely advection condition. The analytical results are obtained with the first and second order approximations ([10], [36]):

- in the longitudinal direction,

$$\sigma^2_{\mathrm{L,1st}} = 0.53\,\sigma^2 u_{\mathrm{m}}^2 \quad \text{and} \quad \sigma^2_{\mathrm{L,2nd}} = \sigma^2_{L,\mathrm{1st}} + 0.23\,\sigma^4 u_{\mathrm{m}}^2 \tag{15}$$

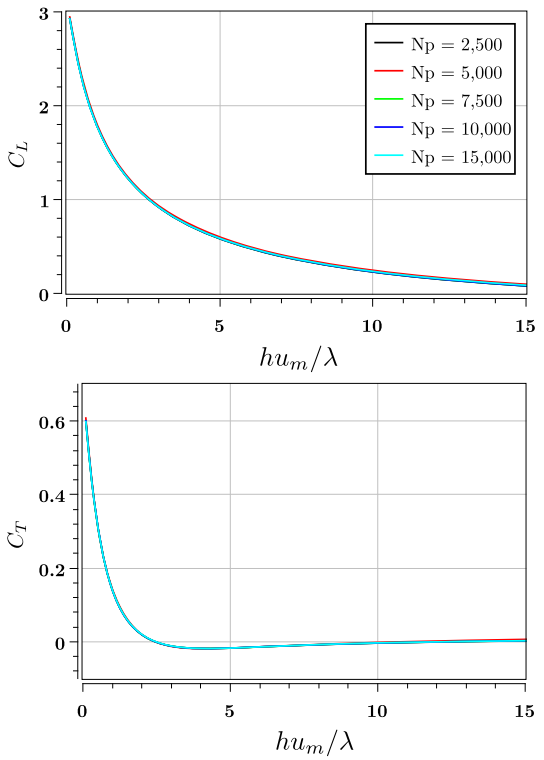

Fig. 2. Longitudinal (C_L, top) and transverse (C_T, bottom) covariance functions obtained with the present method for various values of particle number N_P for a permeability variance $\sigma^2 = 2.25$ with a purely advection condition in 3D.

- in the transverse direction,

$$\sigma^2_{T,1st} = 0.07\,\sigma^2 u^2_m \quad \text{and} \quad \sigma^2_{T,2nd} = \sigma^2_{T,1st} + 0.13\,\sigma^4 u^2_m \tag{16}$$

Fitting curves are used for estimating the relation between the numerical results of Lagrangian velocity variances and the permeability variance σ^2:

- in the longitudinal direction,

$$\sigma^2_{L,fitting} = 0.52\,\sigma^4 \tag{17}$$

- in the transverse direction:

$$\sigma^2_{T,fitting} = 0.075\,\sigma^2 + 0.083\,\sigma^4 \tag{18}$$

For $\sigma^2 < 1$, the present method gives numerical results close to the analytical results obtained with the two approximations. For $1 < \sigma^2 < 2$, the first-order approximation differs, while the second order approximation holds. For $\sigma^2 > 2$, important differences are observed between the present method and the two approximations. Similar comments have already been made by Bellin et al. [37], Salandin et al. [21], and Hassan et al. [38].

4. Covariance function analysis

Fig. 4 shows the longitudinal (C_L, top) and transverse (C_T, bottom) covariance functions in 2D (left) and 3D (right) as functions of time step h for three values of the permeability variance ($\sigma^2 = 0.25$, 1, and 2.25) and three values of the Péclet number ($Pe = 50$, 100, and ∞), obtained with the present method. The Péclet number is defined as $Pe = u_m \lambda / D_m$. The lowest value of Pe taken in this work is limited to 50 when using the covariance function for convergence considerations. For lower values of Pe, the particles leave the computational domain too quickly to correctly sample the Lagrangian velocity. In such cases, the covariance function asymptote does not reach zero.

In the longitudinal direction, a low value of the Péclet number Pe leads to decrease the Lagrangian velocity covariance functions C_L. Russo et al. [34] and Jankovic et al. [39] explain that diffusion allows the particles to sample the areas with high and low permeabilities that would have been unreachable with a purely advection condition. This decrease is further

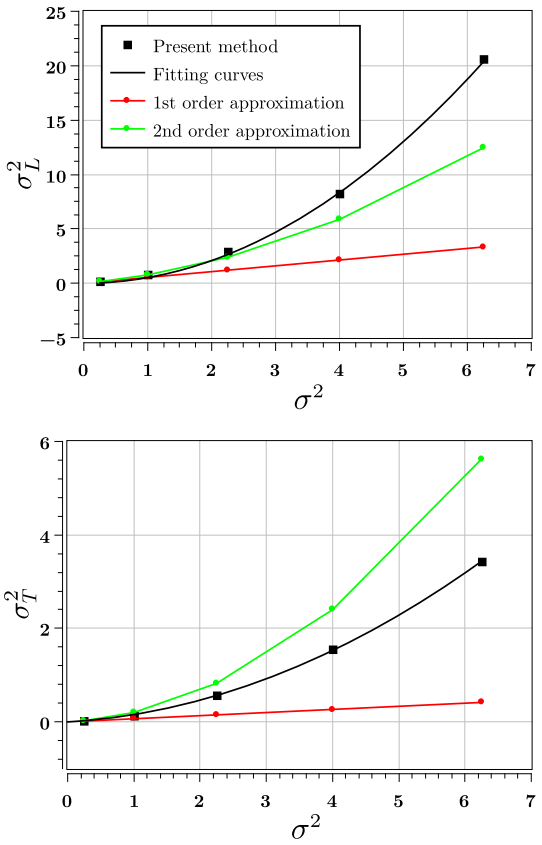

Fig. 3. Longitudinal (σ_L^2, top) and transverse (σ_T^2, bottom) variances of flow velocity fields, as functions of the permeability variance σ^2 with a purely advection condition in 3D (red line: first order approximation given by Dagan [10], green line: second order approximation given by Deng et al. [36], black squares: present method and black line: fitting curves).

reinforced by a high value of the permeability variance σ^2. The same behaviour is found in 2D and 3D. However, the amplification caused by the permeability variance σ^2 is more significant in 3D than in 2D. In the transverse direction, the effect of diffusion on the Lagrangian velocity covariance function C_T is reversed. Hence, a low value of Pe induces a reduction of the negative part of transverse covariance functions C_T. Russo et al. [34] and Jankovic et al. [39] interpret it as an attenuation of perturbations caused by the shift between the convergence and divergence of flow velocity fields in the areas with high and low permeabilities. The amplification with the permeability σ^2 is still observed. But its intensity seems to be identical in 2D and 3D.

Fig. 5 shows the longitudinal ($D_{t,\mathrm{L}}$, top) and transverse ($D_{t,\mathrm{T}}$, bottom) dispersion coefficients in 2D (left) and 3D (right) as functions of time t for the same values of σ^2 and Pe, used in Fig. 4. The dispersion coefficients, adimensionalized by $u_\mathrm{m}\lambda$, are obtained with equation (7), involving the Lagrangian velocity covariance functions, C_L and C_T.

The dispersion coefficients present usual behaviours previously described by Salandin et al. [21], Meyer et al. [40] and Beaudoin et al. [20] under a purely advection condition. After a transient state, $D_{t,\mathrm{L}}$ reaches an asymptotic value $D_{\infty,\mathrm{L}}$, which depends on the permeability variance σ^2 and on the Péclet number Pe. A low value of Pe leads to a smaller asymptotic value if σ^2 is high enough. For $\sigma^2 = 0.25$, the limit of a homogeneous media, where dispersion is entirely dependent on diffusion, starts to appear. The decrease provoked by diffusion is still amplified by σ^2. As observed in Fig. 4, this amplification is more important in 3D than in 2D. $D_{t,\mathrm{T}}$ reaches an early spire followed by a rapid drop toward an asymptotic value $D_{\infty,\mathrm{T}}$. This behaviour can be related to the form of transverse covariance functions C_T as it falls below zero before converging toward it. Furthermore, a low value of Pe induces a higher asymptotic value, while the amplification caused by σ^2 seems to be identical in 2D and 3D.

To further corroborate these assertions, the macroscopic coefficients were also computed by using the moment method ([20]) under a diffusive condition. Moreover, to isolate the contribution of diffusion on dispersion, induced by the effect of diffusion on the sampling of the Eulerian velocity by the particles, the difference ΔD_i ($i = L$ longitudinal and T transverse) is estimated with:

$$\Delta D_i = D_{\infty,i} - D_\mathrm{m} - D^*_{\infty,i} \tag{19}$$

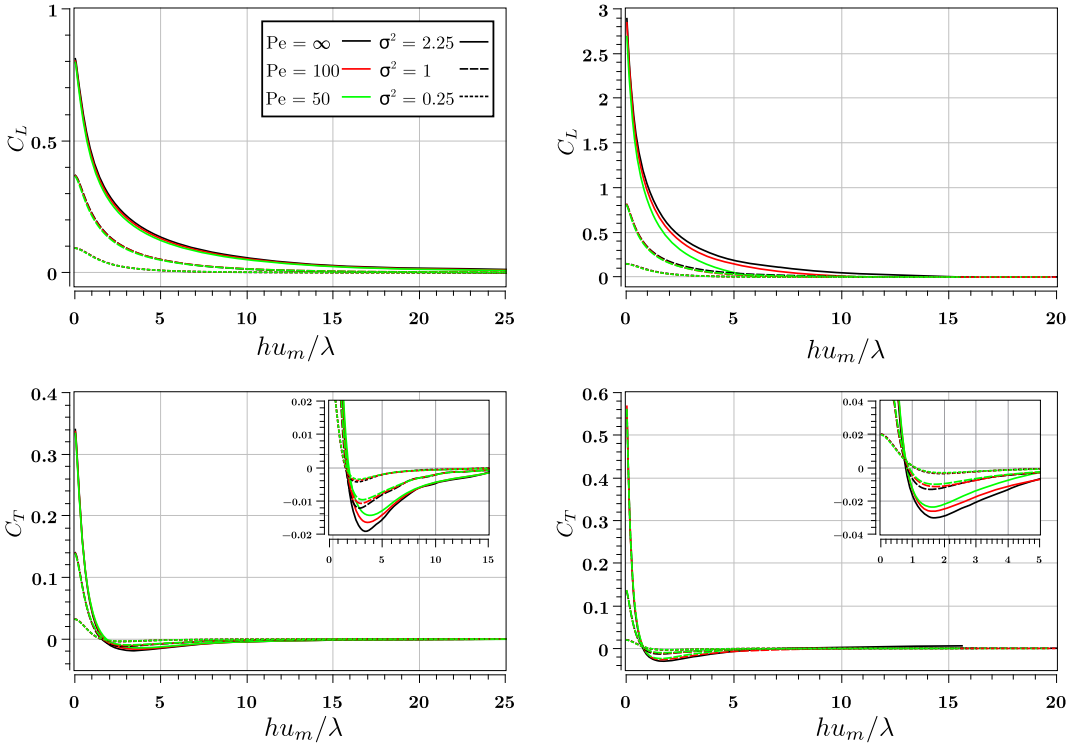

Fig. 4. Longitudinal (C_L, top) and transverse (C_T, bottom) covariance functions in 2D (left) and 3D (right) for various values of the Péclet number (green: $Pe = 50$, red: $Pe = 100$ and black: $Pe = \infty$) and the permeability variance (dotted line: $\sigma^2 = 0.25$, dashed line: $\sigma^2 = 1$ and solid line $\sigma^2 = 2.25$).

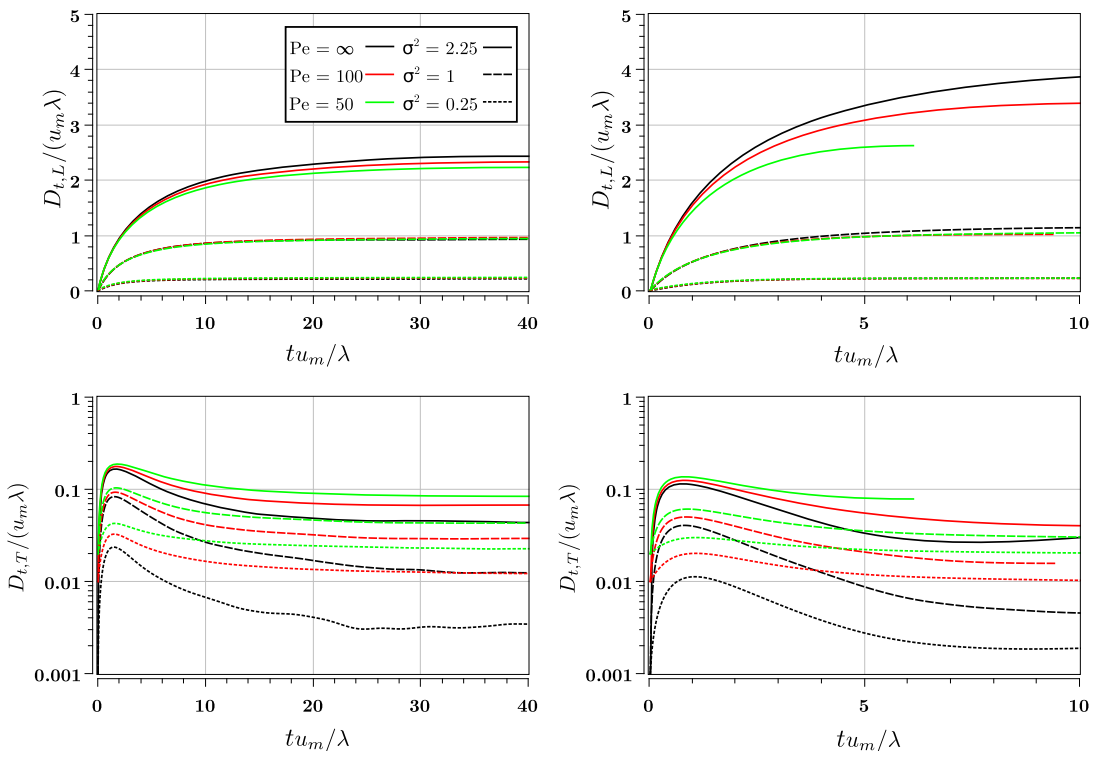

Fig. 5. Longitudinal ($D_{t,L}$, top) and transverse ($D_{t,T}$, bottom) dispersion coefficients, estimated with the equation (7), as functions of time t in 2D (left) and 3D (right) for various values of the Péclet number (green: $Pe = 50$, red: $Pe = 100$ and black: $Pe = \infty$) and the permeability variance (dotted line: $\sigma^2 = 0.25$, dashed line: $\sigma^2 = 1$ and solid line: $\sigma^2 = 2.25$).

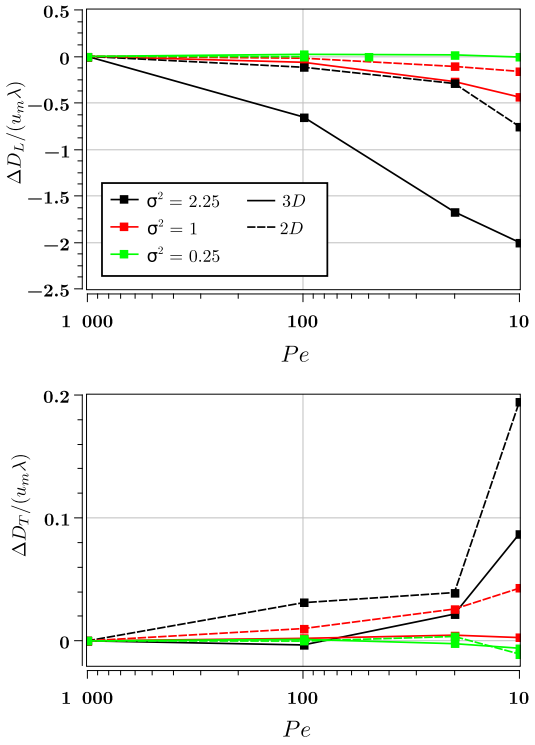

Fig. 6. Difference ΔD_i ($i =$ L, longitudinal (top), and T, transverse (bottom)) as a function of the Péclet number Pe for three values of the permeability variance (green: $\sigma^2 = 2.25$, red: $\sigma^2 = 1$ and black: $\sigma^2 = 0.25$) in 2D (dashed line) and 3D (solid line).

where $D^*_{\infty,i}$ is the asymptotic value $D_{\infty,i}$ with a purely advection condition. The numerical results of ΔD_i have been plotted as functions of the Péclet number Pe in 2D and 3D for the three values of the permeability variance σ^2 used in this work. They are adimensionalized by $u_m\lambda$.

Fig. 6 shows the differences ΔD_i as a function of the Péclet number Pe based on the results of the moments method. The two spatial configurations have the same behaviour with respect to the influence of diffusion on dispersion, a decrease in the longitudinal direction and an increase in the transverse direction. However, the intensity of these two effects depends on the permeability variance σ^2, and is clearly different between the two spatial configurations. In the longitudinal direction, the effect is more pronounced in 3D with a ΔD_L 2.5 times stronger in 3D than in 2D for $Pe = 10$ and $\sigma^2 = 2.25$. In the transverse direction, the highest values of ΔD_T are still reached for the strongest values of σ^2 and the lowest of Pe. However, in 2D, ΔD_T is two times higher than in 3D for $Pe = 10$ and $\sigma^2 = 2.25$. Which can be explained by the fact that molecular diffusion is not the only source of transverse dispersion in 3D. Hence, the effect of diffusion and its amplification by the permeability variance is reduced when compared to the transverse dispersion.

5. Conclusions

The influence of diffusion on dispersion has been highlighted by the Lagrangian velocity covariance function. Moreover, its computation also points out that the effect of diffusion on dispersion varies between 2D and 3D. In the longitudinal direction, the decrease of dispersion induced by diffusion is more strengthened by the permeability variance in 3D than in 2D. In the transverse direction, the increase of dispersion caused by diffusion, is further amplified by the permeability variance in 2D, compared to 3D.

These disparities between 2D and 3D indicate a profound modification of the flow topology generated by the addition of another dimension. The repercussion observed on the covariance function springs from the confinement of streamlines in 2D which prevents inter-crossing ([11], [41]) to the disruption of this same confinement in 3D allowing more complex geometries ([42]). It is indicative of a difference of the flow topology between the 2D and 3D cases. In 2D, the plan flows prevent the streamlines from inter-crossing. Dispersion remains zero in the transverse direction with a purely advection condition. Diffusion breaks this constraint by allowing particles to sample different streamlines. This effect is more pronounced in 2D than in 3D because the 3D flows already generate a transverse dispersion.

References

[1] J. Bear, Dynamics of Fluid in Porous Media, Dover Publications Inc., New York, 1972.

[2] P.G. Saffman, A theory of dispersion in a porous medium, J. Fluid Mech. 6 (1959).
[3] G. Matheron, G. De Marsily, Is transport in porous media always diffusive? A counterexample, Water Resour. Res. 16 (1980) 901–917.
[4] G. Dagan, Stochastic modeling of groundwater flow by unconditional and conditional probabilities, 1. Conditional simulation and the direct problem, Water Resour. Res. 18 (1982) 813–833.
[5] G. Dagan, Stochastic modeling of groundwater flow by unconditional and conditional probabilities, 2. The solute transport, Water Resour. Res. 18 (1982) 835–848.
[6] L.W. Gelhar, C.L. Axness, Three-dimensional stochastic analysis of macrodispersion in aquifers, Water Resour. Res. 19 (1983) 161–180.
[7] C.L. Winter, C.M. Newman, S.P. Neuman, A perturbation expansion for diffusion in a random velocity field, SIAM J. Appl. Math. 42 (1984) 411–424.
[8] G. Dagan, Solute transport in heterogeneous porous formations, J. Fluid Mech. 145 (1984) 151–177.
[9] G. Dagan, Theory of solute transport by groundwater, Annu. Rev. Fluid Mech. 19 (1987) 183–215.
[10] G. Dagan, Flow and Transport in Porous Formations, Springer Verlag, Berlin, Heidelberg, New York, London, Paris, Tokyo, Hong Kong, 1989.
[11] G.I. Taylor, Diffusion by continuous movements, Proc. Lond. Math. Soc. 2 (1921) 196–212.
[12] S.P. Neuman, Y.K. Zhang, A quasi-linear theory of non-Fickian and Fickian subsurface dispersion, 1. Theoretical analysis with application to isotropic media, Water Resour. Res. 26 (1990) 887–902.
[13] S. Attinger, M. Dentz, W. Kinzelbach, Exact transverse macro dispersion coefficients for transport in heterogeneous porous media, Stoch. Environ. Res. 18 (2004) 9–15.
[14] A. Fiori, Finite Peclet extensions of Dagan's solutions to transport in anisotropic heterogeneous formation, Water Resour. Res. 32 (1996) 193–198.
[15] A. Chaudhuri, M. Sekhar, Analytical solutions for macrodispersion in a 3D heterogeneous porous medium with random hydraulic conductivity and dispersivity, Transp. Porous Media 58 (2005) 217–241.
[16] H. Schwarze, U. Jaekel, H. Vereecken, Estimation of macrodispersion by different approximation methods for flow and transport in randomly heterogeneous media, Transp. Porous Media 43 (2001) 265–287.
[17] M. Dentz, H. Kinzelbach, S. Attinger, W. Kinzelbach, Temporal behavior of a solute cloud in a heterogeneous porous medium: 3. Numerical simulations, Water Resour. Res. 38 (7) (2002) 23-1–23-13.
[18] M. Trefry, F. Ruan, D. McLaughlin, Numerical simulations of preasymptotic transport in heterogeneous porous media: departures from the Gaussian limit, Water Resour. Res. 39 (3) (2003).
[19] I. Jankovic, A. Fiori, G. Dagan, Modeling flow and transport in highly heterogeneous three-dimensional aquifers: ergodicity, gaussianity, and anomalous behavior: 1. Conceptual issues and numerical simulations, Water Resour. Res. 42 (6) (2006).
[20] A. Beaudoin, J.R. de Dreuzy, Numerical assessment of 3D macrodispersion in heterogeneous porous media, Water Resour. Res. 49 (2013) 1–8.
[21] P. Salandin, V. Fiorotto, Solute transport in highly heterogeneous aquifers, Water Resour. Res. 34 (1998) 949–961.
[22] H. Gotovac, V. Cvetkovic, R. Andricevic, Flow and travel time statistics in highly heterogeneous porous media, Water Resour. Res. 45 (2009) 1–24.
[23] J.R. de Dreuzy, A. Beaudoin, J. Erhel, Asymptotic dispersion in 2D heterogeneous porous media determined by parallel numerical simulations, Water Resour. Res. 43 (2007) 1–13.
[24] J.R. de Dreuzy, A. Beaudoin, J. Erhel, Reply to comment by A. Fiori et al. on "Asymptotic dispersion in 2D heterogeneous porous media determined by parallel numerical simulations", Water Resour. Res. 44 (2008) 1–2.
[25] A. Beaudoin, J.R. de Dreuzy, J. Erhel, Numerical Monte Carlo analysis of the influence of pore-scale dispersion on macrodispersion in 2D heterogeneous porous media, Water Resour. Res. 46 (2010) 1–9.
[26] A. Englert, J. Vanderborght, H. Vereecken, Prediction of velocity statistics in three-dimensional multi-Gaussian hydraulic conductivity fields, Water Resour. Res. 42 (3) (2006) 1–15.
[27] R. Ababou, D. McLaughlin, L. Gelhar, A.F.B. Tompson, Numerical simulation of three-dimensional saturated flow in randomly heterogeneous porous media, Transp. Porous Media 4 (1989) 549–565.
[28] A.F.B. Tompson, L. Gelhar, Numerical simulation of solute transport in three-dimensional, randomly heterogeneous porous media, Water Resour. Res. 26 (1990) 2541–2562.
[29] D.A. Chin, T. Wang, An investigation of the validity of first-order stochastic dispersion theories in isotropie porous media, Water Resour. Res. 28 (1992) 1531–1542.
[30] B.B. Dykaar, P.K. Kitanidis, Determination of the effective hydraulic conductivity for heterogeneous porous media using a numerical spectral approach, 1. Method, Water Resour. Res. 28 (1992) 1155–1166.
[31] S.P. Neuman, S. Orr, O. Levin, E. Paleologos, Theory and high-resolution finite element analysis of 2-D and 3-D effective permeabilities in strongly heterogeneous porous media, in: Computational Methods in Water Resources IX, 2, 1992.
[32] D.T. Burr, E.A. Sudicky, R.L. Naff, Nonreactive and reactive solute transport in three-dimensional heterogeneous porous media: mean displacement, plume spreading, and uncertainty, Water Resour. Res. 30 (1994) 791–815.
[33] R.L. Naff, D.F. Haley, E.A. Sudicky, High-resolution Monte Carlo simulation of flow and conservative transport in heterogeneous porous media, 1. Methodology and flow results, Water Resour. Res. 34 (1998) 663–677.
[34] D. Russo, On the velocity covariance and transport modeling in heterogeneous anisotropic porous formations, 1. Saturated flow, Water Resour. Res. 31 (1995) 129–137.
[35] G. Severino, R. Campagna, D.M. Tartakovsky, An analytical model for carrier-facilitated solute transport in weakly heterogeneous porous media, Appl. Math. Model. 1 (2017) 1–13.
[36] F.W. Deng, J.H. Cushman, On higher-order corrections to the flow velocity covariance tensor, Water Resour. Res. 31 (1995) 1659–1672.
[37] A. Bellin, P. Salandin, A. Rinaldo, Simulation of dispersion in heterogeneous porous formations: statistics, first-order theories, convergence of computations, Water Resour. Res. 28 (1992) 2211–2227.
[38] A.E. Hassan, J.H. Cushman, J.W. Delleur, A Monte Carlo assessment of Eulerian flow and transport perturbation models, Water Resour. Res. 34 (1998) 1143–1163.
[39] I. Jankovic, A. Fiori, G. Dagan, Flow and transport in highly heterogeneous formations, 3. Numerical simulations and comparison with theoretical results, Water Resour. Res. 39 (2003) 1–12.
[40] D.W. Meyer, H.A. Tchelepi, Particle-based transport model with Markovian velocity processes for tracer dispersion in highly heterogeneous porous media, Water Resour. Res. 46 (2010) 1–22.
[41] V. Cvetkovic, H. Cheng, X.H. Wen, Analysis of nonlinear effects on tracer migration in heterogeneous aquifers using Lagrangian travel time statistics, Water Resour. Res. 32 (1996) 1671–1680.
[42] M. Bakker, K. Hemker, Analytic solutions for groundwater whirls in box-shaped, layered anisotropic aquifers, Adv. Water Resour. 27 (2004) 1075–1086.